

## Spin-dependent electronic structure of the Co/Al(OP)<sub>3</sub> interface

This content has been downloaded from IOPscience. Please scroll down to see the full text.

2013 New J. Phys. 15 113054

(<http://iopscience.iop.org/1367-2630/15/11/113054>)

View [the table of contents for this issue](#), or go to the [journal homepage](#) for more

Download details:

IP Address: 141.3.200.205

This content was downloaded on 29/05/2015 at 09:36

Please note that [terms and conditions apply](#).

## Spin-dependent electronic structure of the Co/Al(OP)<sub>3</sub> interface

Sabine Müller<sup>1</sup>, Sabine Steil<sup>1</sup>, Andrea Droghetti<sup>2</sup>,  
Nicolas Großmann<sup>1</sup>, Velimir Meded<sup>3</sup>, Andrea Magri<sup>3</sup>,  
Bernhard Schäfer<sup>3</sup>, Olaf Fuhr<sup>3</sup>, Stefano Sanvito<sup>2</sup>, Mario Ruben<sup>3</sup>,  
Mirko Cinchetti<sup>1,4</sup> and Martin Aeschlimann<sup>1</sup>

<sup>1</sup> Department of Physics and Research Center OPTIMAS, University of Kaiserslautern, Erwin-Schrödinger-Strasse 46, D-67663 Kaiserslautern, Germany

<sup>2</sup> School of Physics and CRANN, Trinity College Dublin, Dublin 2, Ireland

<sup>3</sup> Institute of Nanotechnology, Karlsruhe Institute of Technology, D-76344 Eggenstein-Leopoldshafen, Germany

E-mail: [cinchetti@rhrk.uni-kl.de](mailto:cinchetti@rhrk.uni-kl.de)

*New Journal of Physics* **15** (2013) 113054 (12pp)

Received 18 July 2013

Published 26 November 2013

Online at <http://www.njp.org/>

doi:10.1088/1367-2630/15/11/113054

**Abstract.** We have studied the spin-dependent electronic properties of the interface formed between epitaxial Co thin films deposited on Cu(001) and the experimental molecule tris-(9-oxidophenalenone)-aluminum<sup>(III)</sup> (Al(OP)<sub>3</sub>), created as a variation of the prototypical organic semiconductor Alq<sub>3</sub> to tailor the spin filtering properties by modifying chemisorption with cobalt. The interfaces have been grown under ultra-high vacuum conditions by progressive deposition of 0.5–5 nm Al(OP)<sub>3</sub> on the freshly prepared cobalt substrate. For every growth step we have monitored the energy level alignment at the interface as well as the spin polarization of the occupied manifold by spin-resolved photoemission spectroscopy. We identify two hybrid interface states in the energy window of 2 eV below the Fermi energy. The first is at 0.9 eV below  $E_F$  and shows an 8% higher spin polarization than Co, while the second is at 1.6 eV below  $E_F$  and shows a spin polarization reduced by 4%.

<sup>4</sup> Author to whom any correspondence should be addressed.



Content from this work may be used under the terms of the [Creative Commons Attribution 3.0 licence](http://creativecommons.org/licenses/by/3.0/).

Any further distribution of this work must maintain attribution to the author(s) and the title of the work, journal citation and DOI.

Organic semiconductors constitute a very promising material class for spintronics applications [1]. The interest in the spin properties of organic semiconductors was originally stimulated by the observation of magneto-resistive effects in spin-valve structures prepared with an organic-based spacer [1–3]. Recently, it has become clear that the performance of such organic spintronic devices is strongly determined by the peculiar spin-dependent properties of the hybrid interface formed between the organic semiconductor and the ferromagnetic electrodes [4, 5]. Such *spinterfaces* [6] constitute indeed a new playground for exploiting the spin properties of organic materials, as they can be potentially used both as tunable spin filters [7] with enhanced or even inverted spin polarization (SP) with respect to the ferromagnetic electrodes [4] or as independent supramolecular layers showing interface magneto-resistive effects [8].

Co/Alq<sub>3</sub> is the prototypical spinterface, as it constitutes the basic building block of a large number of organic spintronics devices [1]. Recent spin- and time-resolved spectroscopy experiments have revealed the existence of spin polarized hybrid interface states (HISs) at the Co/Alq<sub>3</sub> interface, which act microscopically as spin traps and thus determine the spin-filtering properties of the Co/Alq<sub>3</sub> interface [11]. Moreover, different recent works suggest that spinterfaces formed by Alq<sub>3</sub> can be easily tuned to control the spintronic performance of organic spin valves [9, 10]. Another intriguing pathway to tailor the spin properties of the Co/Alq<sub>3</sub> interface, and thus to directly control and tune the performance of the related devices, is to systematically engineer the electronic properties of Alq<sub>3</sub> by chemical substitution. Different electronic properties of the molecule will inevitably lead to a modified interaction (in character and strength) between the molecule and the ferromagnetic substrate, and thus to modified spin filtering properties of the spinterface.

This is the approach that we propose in this paper. We make use of the mutability of organic semiconductors [12] to create the experimental molecule tris-(9-oxidophenalenone)-aluminum<sup>(III)</sup> (Al(OP)<sub>3</sub>) as a variation of the aromate Alq<sub>3</sub>. Al(OP)<sub>3</sub> was developed to produce a molecule that has bigger ligands than Alq<sub>3</sub>. We expect a modification of the chemisorption on cobalt, and thus different spin-dependent properties of the Co/Al(OP)<sub>3</sub> spinterface with respect to Co/Alq<sub>3</sub>. After having introduced the molecular system, we present a systematic characterization of the spin-dependent properties of the Co/Al(OP)<sub>3</sub> interface by spin-dependent spectroscopy and compare them with the well-known properties of Co/Alq<sub>3</sub>. Our spectroscopic studies are corroborated by density functional theory (DFT) calculations. This study thus provides a full characterization of the Co/Al(OP)<sub>3</sub> system which we propose as a first step toward chemical functionalization of spinterfaces for organic spintronics applications.

The synthesis of Al(OP)<sub>3</sub> was carried out as previously described [13] (see the [appendix](#)). In order to achieve high purity of the material, several purification steps such as column chromatography and recrystallization by solvent slow evaporation were performed, purity was checked stepwise by common analysis techniques such as nuclear magnetic resonance (NMR) spectroscopy, mass spectrometry (matrix-assisted laser desorption/ionization time-of-flight experiment (MALDI-TOF)) and elemental analysis. Single crystals of the compounds were obtained, the molecular structure was resolved by x-ray single-crystal diffraction for the first time (see figure 1) and therefore reported (see the [appendix](#), further details can be found in the Cambridge Crystallographic Data Centre, reference number: CCDC 963395). The atoms' coordinates could be extrapolated from the x-ray single-crystal diffraction and were used as the starting point for DFT optimization of the molecule structure in 'gas phase'.

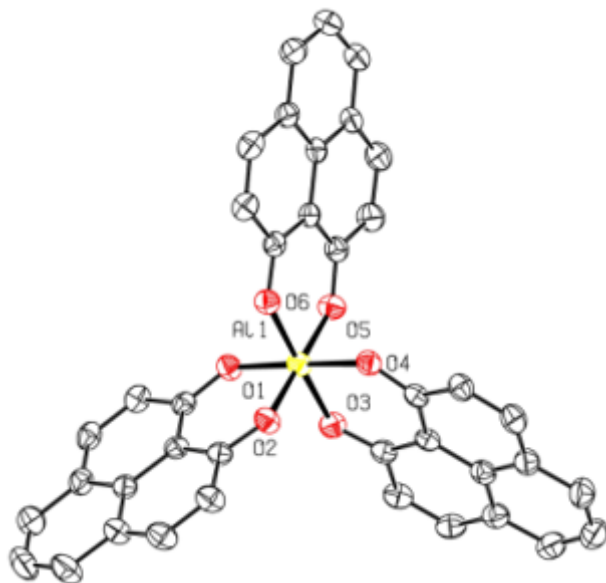


**Figure 1.** Molecular structure of  $\text{Al(OP)}_3$  (hydrogen atoms and solvent molecules are omitted for clarity).

As a first step to the characterization of the spin-dependent properties of  $\text{Co/Al(OP)}_3$ , we study here the interface formed between epitaxial Co thin films deposited on  $\text{Cu(001)}$  and  $\text{Al(OP)}_3$ . The organic molecule was progressively grown on a freshly deposited cobalt thin film with coverage ranging between 0.5 and 5 nm. The occupied manifold of the interface was characterized by spin-resolved ultraviolet photoemission spectroscopy (UPS). For every growth step, we monitored the changes in the work function and the energetic position of the molecular orbitals, giving information about the energy level alignment, the SP and the origin of the electronic states of the interface.

All of the spectroscopic measurements were performed with an UHV-system consisting of one spectrometer chamber and two evaporator chambers. The base pressure in the spectrometer chamber is  $4 \times 10^{-11}$  mbar. The evaporator chambers enable us to produce the  $\text{Co/Al(OP)}_3$  system *in situ*, which is crucial to obtain a clean surface and a high-quality interface. Cobalt is evaporated by an Omicron EFM 3 evaporator at a pressure of  $10^{-10}$  mbar.  $\text{Al(OP)}_3$  is deposited with a Knudscell from Kentax GmbH evaporator at a pressure of  $9 \times 10^{-10}$  mbar. The deposition rates are monitored by a quartz crystal balance calibrated with ellipsometry.

The 3.5 nm thin Co films were deposited by electron beam epitaxy on a  $\text{Cu(001)}$  single crystal. Afterwards, the substrate was annealed at 370 K. This results in a metastable tetragonally distorted Co fcc structure with in-plane magnetic uniaxial anisotropy along the (110) direction of copper [15, 16]. The  $\text{Co/Cu(001)}$  film was then progressively covered with  $\text{Al(OP)}_3$ , to form the  $\text{Co/Al(OP)}_3$  interface.

To detect the occupied manifold of the  $\text{Co/Al(OP)}_3$  system, we performed UPS and near threshold photoemission spectroscopy (NT-PS) [17, 18]. UPS was performed by using an Omicron HIS 13 vacuum ultraviolet lamp, which operates at the HeI line ( $h\nu = 21.2$  eV). The excitation source for NT-PS is a Ti:sapphire laser system with a central wavelength of 800 nm, 82 MHz repetition rate, a pulse power of 1.5 W and a pulse duration of 100 fs. The output is frequency quadrupled by using two beta-barium borate crystals leading to the fourth

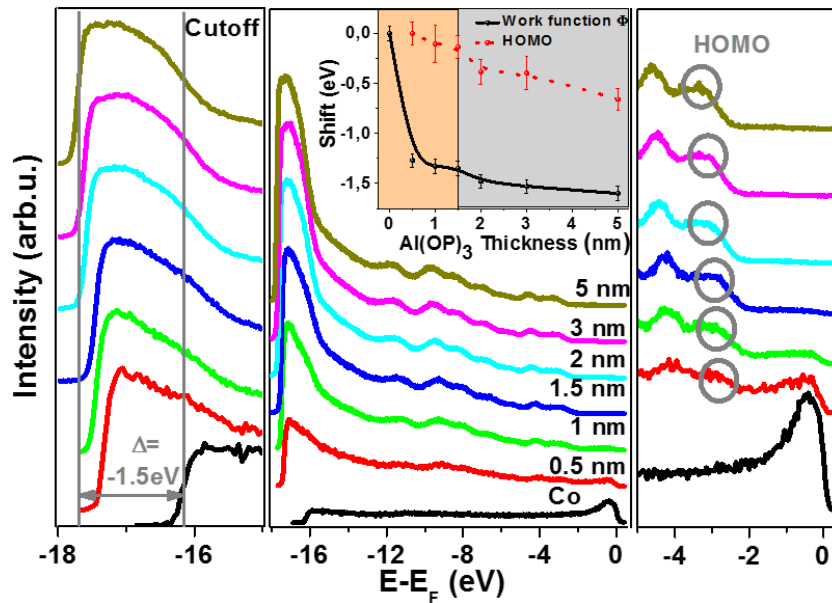


**Figure 2.** UPS spectra of the Co/[ $x$  nm]Al(OP)<sub>3</sub> system with  $x = 0$  nm (Co substrate), 0.5, 1, 1.5, 2, 3 and 5 nm. The right panel shows the UPS spectra in the HOMO region magnified for more detail. The HOMO (marked with a circle) shifts to lower energies for increasing  $x$ . The right panel shows the region of the low-energy cutoff; here the UPS spectra have been normalized to 1. The maximal energetic shift of the low-energy cutoff ( $\Delta = -1.5$  eV) is also marked. Inset: shift of the work function (black) and shift of the HOMO (red, dashed) versus Al(OP)<sub>3</sub> coverage. Cobalt work function is 5.1 eV, energetic position of the HOMO for  $x = 5$  nm is  $-3.3$  eV.

harmonic of the fundamental with a photon energy of 5.95 eV. For both the UPS and the NT-PS the light incident angle was  $45^\circ$ . The emitted photoelectrons are energy and spin selected by a spin detector based on spin polarized low-energy electron diffraction (Focus SPLEED) mounted on a commercial cylindrical sector analyzer (Focus CSA). The acceptance angle of the detector system is  $\pm 13^\circ$  and its energy resolution is 0.22 eV. All of the presented measurements were performed at room temperature.

Figure 2 shows the UPS spectra of the Co/[ $x$  nm]Al(OP)<sub>3</sub> system for  $x = 0.5, 1, 1.5, 2, 3$  and 5 nm. The left panel of figure 2 shows the low-energy cutoff of the UPS spectra, with maximum intensity normalized to 1. From the position of the cutoff ( $E_{\text{cutoff}}$ ) we can extract the work function  $\Phi = (21.2 - E_{\text{cutoff}})$  eV. The change in work function with increasing Al(OP)<sub>3</sub> coverage extracted from the UPS spectra is depicted in the inset of figure 2. We observe a reduction of the work function  $\Phi$  with increasing Al(OP)<sub>3</sub> coverage up to 1.5 nm. This reduction is caused by a negative interface dipole with strength  $\Delta = -1.5$  eV. This value is virtually identical to the interface dipole observed for the Co/Alq<sub>3</sub> system [11]. Note that the work function is almost constant for coverage above 1.5 nm (indicated by the vertical line in the graph), suggesting that at this nominal coverage the Co is completely covered by Al(OP)<sub>3</sub> molecules [19, 20]. We thus define 1 monolayer Al(OP)<sub>3</sub> as the nominal thickness of 1.5 nm.

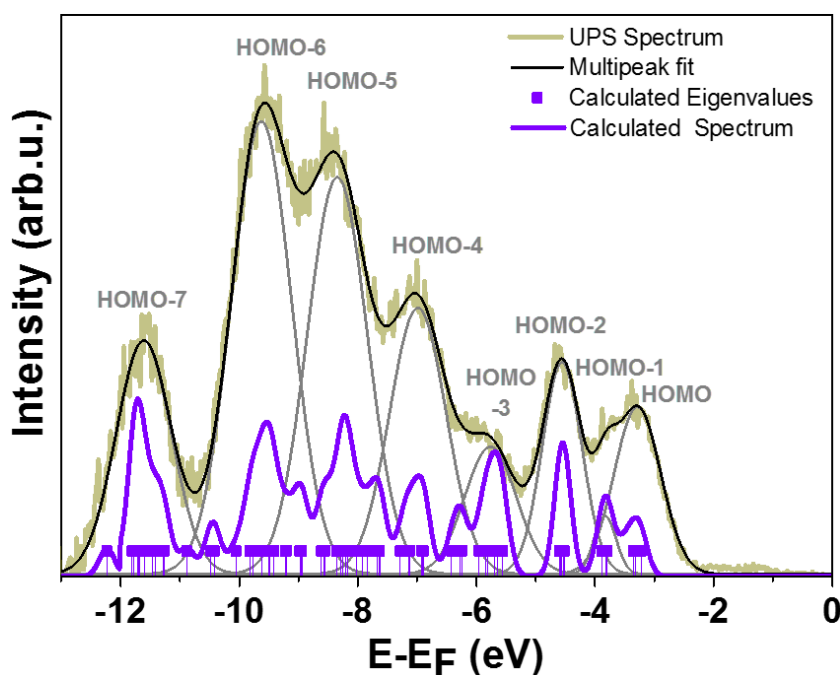


**Figure 3.** UPS spectrum of the Co/[5 nm]Al(OP)<sub>3</sub> system after subtraction of the inelastic electron background function performed according to [22] (brown). The spectrum is fitted with an eight-peak function (black) providing the energetic position of eight occupied states of Al(OP)<sub>3</sub> (gray: HOMO, HOMO-1, ..., HOMO-7). The purple vertical bars indicate the energy of the generalized eigenvalues calculated with DFT-B3LYP, while the purple continuous lines represent the density of states with a Gaussian broadening of 0.22 eV to include the inhomogeneous broadening originating from the instrumental resolution.

The right panel of figure 2 shows the UPS spectra in the region of the highest occupied molecular orbital (HOMO) magnified for more detail. We observe a progressive shift of the HOMO of the Co/Al(OP)<sub>3</sub>-system toward lower energies with increasing Al(OP)<sub>3</sub> coverage. The shift is plotted in the inset as a dashed red line. The HOMO position ranges from  $-2.6$  eV at  $x = 0.5$  nm to  $-3.3$  eV at  $x = 5$  nm, and shifts almost linearly as a function of Al(OP)<sub>3</sub> coverage. In contrast to the work function, the HOMO position does not remain constant for coverage above 1.5 nm. The shift in energy of the HOMO position is most probably due to the different conditions experienced by the Al(OP)<sub>3</sub> molecules in a submonolayer, a monolayer, a bulk molecular film and at the surface of a molecular film, as described by Hill *et al* [21]. In particular, the surrounding potential of the cobalt film of the neighboring molecules and of the vacuum will vary with coverage. As the UPS is surface sensitive, the UPS spectra contain mainly information about the first monolayer of the organic molecules. However, for 2 and 3 nm Al(OP)<sub>3</sub> coverage the spectra contain a non-vanishing contribution from the Co/Al(OP)<sub>3</sub> interface (the cobalt Fermi edge is still slightly visible in the UPS spectra), while for the 5 nm coverage we mainly detect the surface of the molecular film, with contributions from the underlying molecules in the bulk.

Figure 3 shows the UPS spectrum of the Co/[5 nm]Al(OP)<sub>3</sub> system after subtraction of the inelastic electron background function given by Henrich *et al* [22]. By approximating the

spectrum with a multi-peak function, we determined eight occupied states of  $\text{Al}(\text{OP})_3$ . Their energetic position is listed in the table in figure 6. As already mentioned, at 5 nm  $\text{Al}(\text{OP})_3$  coverage, electrons originating from the Co and from the Co/ $\text{Al}(\text{OP})_3$  interface cannot be photoemitted anymore, since in the UPS experiment their mean free path is considerably smaller than 5 nm. This means that the molecular orbitals determined by the UPS from the Co/[5 nm] $\text{Al}(\text{OP})_3$  system can be compared with the occupied manifold of a free  $\text{Al}(\text{OP})_3$  molecule. As, to our knowledge, neither experimental nor theoretical studies about free  $\text{Al}(\text{OP})_3$  have been reported, we have performed DFT calculations in order to obtain some insight into its electronic structure.

The DFT calculations were carried out with the NWCHEM [23] and the Turbomole [24, 25] quantum chemistry package. The hybrid exchange correlation functional B3LYP [26] was employed together with the 6-31G\* basis sets, which gives well converged results for all of the quantities of interest. B3LYP and other hybrid functionals have been employed successfully in the description of the free  $\text{Alq}_3$  molecule [27, 28] and, in that case, the density of states compares quantitatively with the UPS spectrum [28, 29]. Furthermore, hybrid functionals often improve the description of molecular spectra by partially correcting for the inherent self-interaction error of local and semi-local functionals [30].

The geometry optimization of the free molecule was carried out in two different ways: firstly, without imposing any symmetry (and using as initial condition the experimental condensed phase geometry) and, secondly, by requiring the molecule coordinates to transform according to the  $C_3$  point group. The results of both optimizations were found to be consistent and the computed Al–O bond lengths are 1.89 Å, a value that is almost identical to that obtained for the Al–O bonds in  $\text{Alq}_3$  [27]. We note that only minor differences between the computed geometry of the free molecule and the experimental geometry of the molecule in the crystalline phase were found. Furthermore, most of the electronic properties (HOMO–LUMO gap (LUMO: lowest occupied molecular orbital), dipole moment, etc) are predicted to be virtually identical (within the numerical uncertainties of our calculations) for the two cases.

The HOMO energy can be computed accurately by using the  $\Delta\text{SCF}$  method [31] and it is found to be equal to  $-6.6$  eV. This result is in good agreement with the HOMO position (with respect to the vacuum energy) inferred from the UPS spectra of the Co/[5 nm] $\text{Al}(\text{OP})_3$  system. In fact, as shown in figure 6, this is about  $-6.9$  eV. Similarly, through the  $\Delta\text{SCF}$  method, the LUMO is calculated to be at  $-1.25$  eV and the transport gap is then equal to 5.35 eV, i.e. about 0.5 eV smaller than the computed  $\text{Alq}_3$  transport gap [27].

The DFT-B3LYP spectrum superimposed on the UPS spectrum of the Co/[5 nm] $\text{Al}(\text{OP})_3$  system is also displayed in figure 3 (purple). Since the generalized eigenvalue corresponding to the HOMO is at  $-5.57$  eV (i.e. about 1 eV higher in energy than the experimental HOMO position with respect to the vacuum energy), the entire theoretical spectrum was first displaced in order to align the HOMO eigenvalue with the  $\Delta\text{SCF}$  HOMO and then shifted so that the 0 eV energy coincided with the Co Fermi energy. By doing that, fairly good agreement between the experimental and the theoretical spectra is obtained. The eight-peak structure is clearly recognizable, although some differences between theoretical and experimental results are present. These are mainly visible in the region between  $-5$  and  $-7$  eV, where the theoretical spectrum presents two symmetric peaks with a small extra feature in between, while the UPS spectrum presents a sharp peak besides a broader shoulder (called, respectively, HOMO-4 and HOMO-3). The origin of this difference between the DFT and the UPS spectra is not clear yet and a complete understanding of the problem would require comparison between various

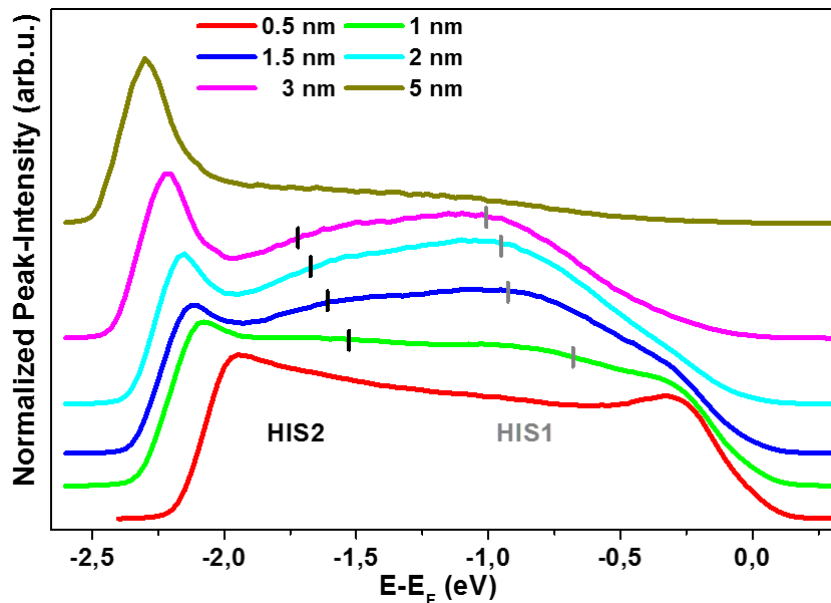


**Figure 4.** Normalized NT-PS spectra of the Co/[ $x$  nm]Al(OP)<sub>3</sub> system with 0.5, 1, 1.5, 2, 3 and 5 nm. The energetic positions of the two interface states HIS1 and HIS2, detectable for  $1 \leq x \leq 3$  nm are marked in the spectra.

computational schemes. However, this goes beyond the goals of this work and it may be considered in future studies.

Interestingly, in Al(OP)<sub>3</sub> the ligands solely bind to the Al<sup>3+</sup> ion via oxygen donor atoms in the chelating moiety. In contrast, in Alq<sub>3</sub>, oxygen and nitrogen atoms connect to the metal ion in symmetrically non-equivalent positions. As a consequence, the calculated vacuum molecular dipole of Al(OP)<sub>3</sub> turns out to be very small when compared to Alq<sub>3</sub>, namely 0.5 versus 4.1 Debye. Experimentally, spinterface dipole moments of Al(OP)<sub>3</sub> and Alq<sub>3</sub> are virtually identical ( $\Delta = 1.5$  eV, see figure 6), which points to the fact that the interface facilitates symmetry breaking. The symmetry can be broken due to at least two distinct mechanisms: firstly, interface charge transfer and hybridization and secondly, by substantial environment symmetry lowering. The low symmetry of the environment, in its turn, can break the internal symmetry of the molecule, resulting in significant increase of the intrinsic molecular dipole. Moreover, we would like to point out that the value of the spinterface dipole is also strongly influenced by changes in the interface charge density induced by the hybridization between Al(OP)<sub>3</sub> and cobalt.

We now proceed in discussing the NT-PS experiments. Figure 4 shows the normalized NT-PS spectra for the Co/[ $x$  nm]Al(OP)<sub>3</sub> system. In the spectra, three features are visible. The first spectroscopic feature close to  $E_F$  arises from excitation of a cobalt bulk state with  $\Delta 5$  symmetry [16]. Accordingly, its intensity decreases for increasing Al(OP)<sub>3</sub> coverage and has almost vanished already at  $x = 2$  nm. Two further features are visible in the spectra for coverage up to 3 nm. Those two features are only present in the spectra for coverage between 0.5 and 3 nm, and disappear at  $x = 5$  nm. This means that with NT-PS we detect two HISs, forming at the Co/Al(OP)<sub>3</sub> interface. This confirms the recent observation that the NT-PS performed on hybrid systems consisting of a metallic underlayer and a non-metallic top layer is highly sensitive to the metal–non-metal interface [32].

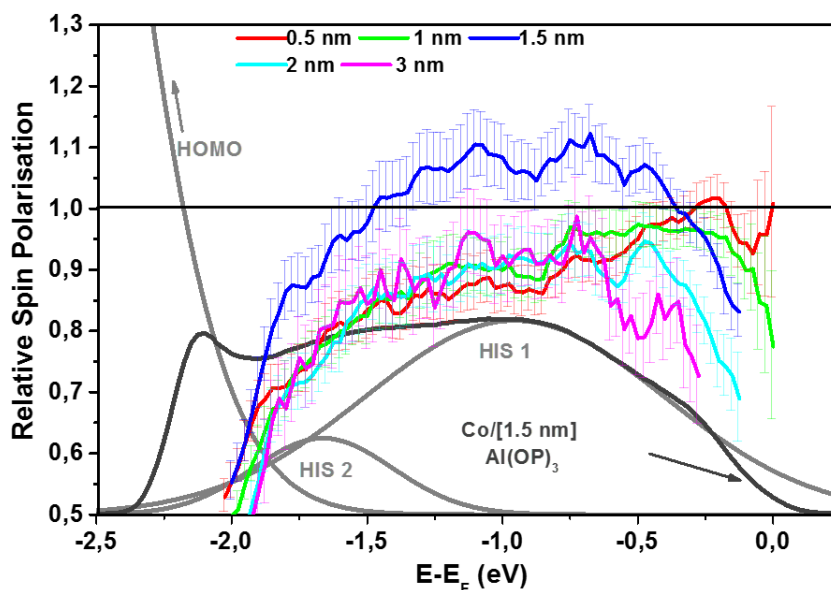


**Figure 5.** Multi-peak fit used to extract the energetic position of HIS1 and HIS2 states, exemplarily shown for the NT-PS spectrum of the Co/[1.5 nm]Al(OP)<sub>3</sub> system. HIS1 and HIS2 are variables in the multi-peak function while the HOMO is at the energetic position extracted from the UPS spectra. The right y-axis indicates the relative SP of the Co/[*x* nm]Al(OP)<sub>3</sub> system, calculated as the ratio between the SP of the Co/[*x* nm]Al(OP)<sub>3</sub> and the SP of cesiated Cobalt (CsCo), measured by spin-resolved NT-PS.

In order to extract the exact energetic position of the two HISs, we performed a multi-peak fit as illustrated in figure 5 exemplarily for the  $x = 1.5$  nm spectrum. In the fit, the position of the two peaks is a variable in the multi-peak function, while the photoemission intensity at the low-energy cutoff, arising from the Al(OP)<sub>3</sub> HOMO, is modeled by a further peak at the energetic position determined with the UPS experiments. The energetic positions of the two HISs, extracted from the multi-peak fit, are marked in figure 4 by vertical lines. The two states are named HIS1 and HIS2, respectively. In analogy with the HOMO of Al(OP)<sub>3</sub>, the energetic position of the two interface states shifts to lower energy with increasing coverage of Al(OP)<sub>3</sub>, which we interpret again as a result of the interaction of these states with the surrounding potential of Co, the neighboring molecules and the vacuum [21].

In the following, we evaluate and discuss the SP of the detected HISs. To be able to compare the SP of Co with that of the HISs over the complete energy range of the NT-PS measurements, we used cesium to lower the work function of cobalt. It is known that cesium does not influence significantly the SP of cobalt [16]. The SP measured by the NT-PS from the cesiated cobalt sample (CsCo in the following) ranges between 30 and 40%, in agreement with [16, 33]. Figure 5 shows the relative SP measured by the NT-PS from the Co/[*x* nm]Al(OP)<sub>3</sub> system for  $x = 0.5, 1, 1.5, 2$  and  $3$  nm. The relative SP is calculated by normalizing the SP of Co/[*x* nm]Al(OP)<sub>3</sub> to the SP of CsCo, determined previously on a different cobalt sample. The relative SP gives thus a measure of the variation of the Co SP when the Co/Al(OP)<sub>3</sub> spinterface is formed. We observe that the relative SP for  $x = 1.5$  nm deviates from the SP measured at the other Al(OP)<sub>3</sub> coverage; it is about 10% higher above

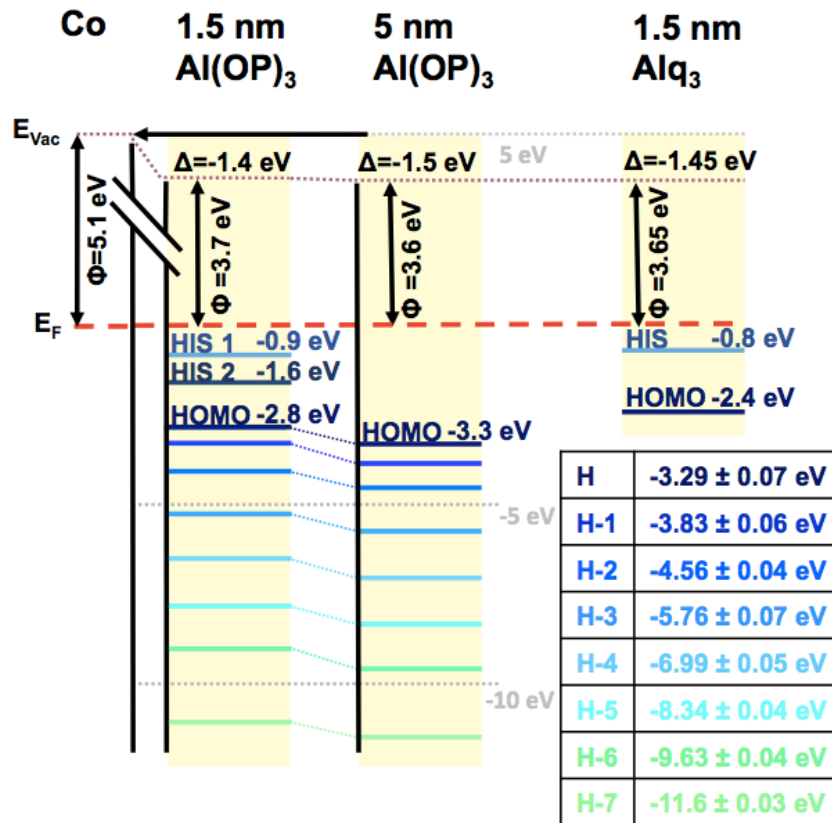


**Figure 6.** Energy level alignment of the Co/[ $x$  nm]Al(OP)<sub>3</sub> system for  $x = 1.5$  and 5 nm compared to the energy level alignment of the Co/Alq<sub>3</sub> interface. The energy level alignment for  $x = 1.5$  nm is extracted from the NT-PS spectra and reflects the alignment of the Co/Al(OP)<sub>3</sub> spinterface. The alignment for  $x = 5$  nm reflects the occupied manifold of bulk Al(OP)<sub>3</sub> and is extracted from the UPS spectra. The alignment at the Co/Alq<sub>3</sub> interface is taken from [11].

the whole energetic range. Note that at  $x = 1.5$  nm we are mostly sensitive to the Co/Al(OP)<sub>3</sub> spinterface, and thus we detect the true spinterface SP. In fact, for  $x < 1.5$  nm the interface dipole and therefore the HISs are not completely formed and thus their spectral weight is very low. For  $x > 1.5$  nm, in turn, the spectral weight of the spin-polarized electrons originating from the spinterface is much lower than the spectral weight of the unpolarized electrons excited from the HOMO in bulk Al(OP)<sub>3</sub>. This artificially reduces the value of the detected SP of the HIS2 state, which decreases much more strongly with increasing Al(OP)<sub>3</sub> thickness than the SP of the HIS1 state. The measured SP of both HIS states is artificially reduced with increasing Al(OP)<sub>3</sub> thickness also as a consequence of the spin-flip processes experienced (in the final state for photoemission) by the spin-polarized electrons photoexcited at the Co/Al(OP)<sub>3</sub> interface while they travel through the Al(OP)<sub>3</sub> layer before being photoemitted.

We now analyze in detail the behavior of the relative SP for  $x = 1.5$  nm, i.e. the Co/Al(OP)<sub>3</sub> spinterface SP. At the energetic position of the HIS1, the relative SP is above 100%, up to 10% higher than the SP of Co. Averaged over the energetic region of HIS1 we observe an enhancement of the SP of 8%. At the energetic position of the HIS2, the relative SP

is below 100%, on average 4% lower than the SP of Co. We thus conclude that the HIS1 has an SP parallel to the cobalt magnetization, while the HIS2 is either unpolarized or polarized antiparallel to the cobalt magnetization.

In conclusion, we investigated the Co/[ $x$  nm]Al(OP)<sub>3</sub> system by spin-dependent photoemission spectroscopy. Our findings are summarized in figure 6: the left part shows the energy level alignment for  $x = 1.5$  nm, which is extracted from the NT-PS spectra and reflects the alignment of the Co/Al(OP)<sub>3</sub> spinterface. The spinterface electronic structure near  $E_F$  is dominated by two HISs, HIS1 and HIS2. HIS1 is located at  $E - E_F = -0.9$  eV and shows on average a 8% higher SP than the Co surface. HIS2 is located at  $E - E_F = -1.6$  eV and shows on average an SP of 4% lower than the SP of cobalt. The middle part of figure 6 shows the energy level alignment at the Al(OP)<sub>3</sub> coverage of  $x = 5$  nm, i.e. bulk Al(OP)<sub>3</sub>. We determined eight occupied states of Al(OP)<sub>3</sub> and an interface dipole of  $\Delta = -1.5$  eV. For comparison to the Co/Alq<sub>3</sub> system, in the right part of figure 6 we present the energy level alignment reported from the Co/Alq<sub>3</sub> interface in [11]. As already discussed the interface dipoles are virtually identical, and moreover, the position of the HOMO is quite similar:  $-2.8$  eV for Al(OP)<sub>3</sub> and  $-2.4$  eV for Alq<sub>3</sub>. However, the HISs formed for the two molecules are crucially different: two states at the Co/Al(OP)<sub>3</sub> interface versus one state at the Co/Alq<sub>3</sub> interface. Besides providing a full characterization of the spin-dependent electronic properties of the Co/Al(OP)<sub>3</sub> system, our results thus also demonstrate the success of the chemical tailoring approach proposed for the engineering of spinterfaces.

## Acknowledgments

The research leading to these results was partly funded by the SFB/TRR 88 ‘3MET’ from the DFG and by the EU project NMP3-SL-2011-263104 ‘HINTS’. VM acknowledges financial support of the FP7-infrastructure project MMM@HPC EC and the joint STFC-DFG project MODEOLED.

## Appendix. Synthesis and characterization of Al(OP)<sub>3</sub>

All of the reactions were carried out under argon inert atmosphere using standard Schlenk techniques. All of the chemicals are commercially available and were used without any further purification, toluene was distilled over Na. <sup>1</sup>H and <sup>13</sup>C NMR spectroscopic data were recorded on a 500 MHz NMR spectrometer with solvent-proton as internal standard. Mass spectrometric data were acquired by MALDI-TOF experiments with no additional matrix compound other than the sample itself. Elemental analysis was carried out to determine the mass fractions of carbon and hydrogen of the sample. 9-Hydroxyphenalenone (1.0203 g, 5.2 mmol) was dissolved in 50 ml of freshly distilled toluene, aluminum chloride (0.2134 g, 1.6 mmol) was added and the solution was refluxed overnight at 110 °C. The yellow precipitate was filtered and washed thoroughly with fresh toluene. The crude product was purified by column chromatography and by recrystallization from CH<sub>2</sub>Cl<sub>2</sub>/CH<sub>3</sub>CH<sub>2</sub>OH yielding to pure yellow powder (0.7673 g, yield 75%). Suitable crystals for single-crystal x-ray diffraction were obtained by slow evaporation of chloroform at room temperature. <sup>1</sup>H NMR (500 MHz, CDCl<sub>3</sub>, 25 °C,  $\delta$ (ppm)): 8.01 (d, 2H,  $J = 9.5$  Hz), 7.96 (d, 2H,  $J = 7.5$  Hz), 7.51 (t, 1H,  $J = 7.5$  Hz) and 7.14 (d, 2H,  $J = 9.0$  Hz). <sup>13</sup>C NMR (125 MHz, CDCl<sub>3</sub>, 25 °C,  $\delta$ (ppm)): 179.09, 141.34, 132.86, 127.94, 127.87, 125.29, 122.91 and 113.40. MALDI-TOF MS (Da):  $m/z$  (rel. intensity, assigned structure) = 416.87

**Table A.1.** Crystallographic and refinement data of  $\text{Al(OP)}_3$  measured at  $T = 180(2)$  K.

Compound	$\text{AlOP}_3 \cdot 3.5\text{CHCl}_3$
Empirical formula	$\text{C}_{42.50}\text{H}_{24.50}\text{AlCl}_{10.50}\text{O}_6$
$M$ ( $\text{g mol}^{-1}$ )	1030.33
Crystal color	Yellow
$\lambda$ ( $\text{\AA}$ )	0.71 073
Crystal system	Monoclinic
Space group	$P2(1)/n$
$a$ (pm)	934.61(4)
$b$ (pm)	2177.32(6)
$c$ (pm)	2133.06(9)
$\beta$ ( $^\circ$ )	90.797(3)
$V$ ( $\text{\AA}^3$ )	4340.2(3)
$Z$	4
$\rho_{\text{calcd.}}$ ( $\text{g cm}^{-3}$ )	1.577
$\mu(\text{Mo} - K\alpha)$ ( $\text{mm}^{-1}$ )	0.742
$F(000)$	2076
Crystal size (mm)	$0.34 \times 0.31 \times 0.30$
$\theta$ range for data collection ( $^\circ$ )	2.13–26.81
Final $R$ indices ( $I > 2\sigma(I)$ )	$R_1 = 0.0609$ , $wR_2 = 0.1589$
$R$ indices (all of the data)	$R_1 = 0.0862$ , $wR_2 = 0.1757$
GoF on $F_2$	1.054

(100%,  $\text{C}_{26}\text{H}_{14}\text{O}_2\text{Al}$  calc. = 417.07). Elemental analysis found (calculated) for  $\text{C}_{39}\text{H}_{27}\text{O}_8\text{Al}$  ( $\text{Al}(\text{C}_{39}\text{H}_{21}\text{O}_6) \cdot 2\text{H}_2\text{O}$ ,  $650.64 \text{ g mol}^{-1}$ ): C 72.29 (71.99)%; and H 4.01 (4.19)%.

Single-crystal x-ray diffraction data were collected on a STOE IPDS II diffractometer with graphite monochromated Mo  $K\alpha$  radiation (0.71 073  $\text{\AA}$ ). Structure solution and refinement against  $F_2$  were carried out by using shelxs and shelxl software [14]. Refinement was performed with anisotropic temperature factors for all of the non-hydrogen atoms (disordered atoms were refined isotropically); hydrogen atoms were calculated on idealized positions. Crystallographic and refinement data of  $\text{Al(OP)}_3$  are summarized in table A.1.

## References

- [1] Dediu V A, Hueso L E, Bergenti I and Taliani C 2009 *Nature Mater.* **8** 707–16
- [2] Xiong Z H, Wu D, Vardeny Z V and Shi J 2004 *Nature* **427** 821–4
- [3] Santos T S, Lee J S, Migdal P, Lekshmi I C, Satpati B and Moodera J S 2007 *Phys. Rev. Lett.* **98** 16601
- [4] Barraud C *et al* 2010 *Nature Phys.* **6** 1–6
- [5] Dediu V A 2013 *Nature Phys.* **9** 210–1
- [6] Sanvito S 2010 *Nature Phys.* **6** 562–4
- [7] Cinchetti M, Neuschwander S, Fischer A, Ruffing A, Mathias S, Wüstenberg J-P and Aeschlimann M 2010 *Phys. Rev. Lett.* **104** 217602
- [8] Raman K V *et al* 2013 *Nature* **493** 509–13
- [9] Prezioso M *et al* 2012 *Adv. Mater.* **25** 534–8

- [10] Schulz L *et al* 2010 *Nature Mater.* **10** 39–44
- [11] Steil S, Großmann N, Laux M, Ruffing A, Steil D, Wiesenmayer M, Mathias S, Monti O L A, Cinchetti M and Aeschlimann M 2013 *Nature Phys.* **9** 242–7
- [12] Naber W J M, Faez S and van der Weil W G 2007 *J. Phys. D: Appl. Phys.* **40** R205–28
- [13] Haddon R C 2002 *US Patent* 6428912
- [14] Sheldrick G M 2008 *Acta Crystallogr.* **A64** 112–22
- [15] Cinchetti M, Heimer K, Wüstenberg J-P, Andreyev O, Bauer M, Lach S, Ziegler C, Gao Y and Aeschlimann M 2009 *Nature Mater.* **8** 115–9
- [16] Andreyev O *et al* 2006 *Phys. Rev. B* **74** 195416
- [17] Cinchetti M, Wüstenberg J-P, Sánchez-Albaneda M, Steeb F, Conca A, Jourdan M and Aeschlimann M 2007 *J. Phys. D: Appl. Phys.* **40** 1544–7
- [18] Fetzer R, Wüstenberg J-P, Taira T, Uemura T, Yamamoto M, Aeschlimann M and Cinchetti M 2013 *Phys. Rev. B* **87** 184418
- [19] Toyoda K, Nakano Y, Hamada I, Lee K, Yanagisawa S and Morikawa Y 2009 *J. Electron Spectrosc. Relat. Phenom.* **147** 78–84
- [20] Shen C and Kahn A 2001 *Org. Electron.* **2** 89–95
- [21] Hill I G, Mäkinen A J and Kafafi Z H 2000 *J. Appl. Phys.* **88** 883–95
- [22] Henrich V E, Li X and Zhang Z 1993 *J. Electron Spectrosc. Relat. Phenom.* **63** 253–65
- [23] Valiev M *et al* 2010 *Comput. Phys. Commun.* **181** 1477–89
- [24] Ahlrichs R, Bär M, Häser M, Horn H and Kölmel C 1989 *Chem. Phys. Lett.* **162** 165
- [25] Häser M and Ahlrichs R 1989 *J. Comput. Chem.* **10** 104
- [26] Becke A D 1993 *J. Chem. Phys.* **98** 5648–52
- [27] Martin R L, Kress J D, Campbell I H and Smith D L 2000 *Phys. Rev. B* **61** 15804–11
- [28] Bisti F, Stroppa A, Donarelli M, Picozzi S and Ottaviano L 2011 *Phys. Rev. B* **84** 195112
- [29] Droghetti A, Pemmaraju C D and Sanvito S 2013 Electronic structure of metal quinoline molecules from G0W0 calculations (in preparation)
- [30] Dori N, Menon M, Kilian L, Sokolowski L, Kronik L and Umbach E 2006 *Phys. Rev. B* **73** 195208
- [31] Jones R O and Gunnarsson O 1989 *Rev. Mod. Phys.* **61** 689–746
- [32] Fetzer R *et al* 2013 Revealing the spin and symmetry properties of the buried Co<sub>2</sub>MnSi/MgO interface by low energy spin-resolved photoemission arXiv:1209.4368
- [33] Steil S, Goedel K, Ruffing A, Sarkar I, Cinchetti M and Aeschlimann M 2011 *Synth. Met.* **161** 570–4